

Seismic fragility of regular masonry buildings for in-plane and out-of-plane failure

Fillitsa Karantoni*, Georgios Tsionis, Foteini Lyrantzaki and Michael N. Fardis

Department of Civil Engineering, University of Patras, 26504 Patras, Greece

(Received September 30, 2013, Revised February 5, 2014, Accepted February 14, 2014)

Abstract. The seismic vulnerability of stone masonry buildings is studied on the basis of their fragility curves. In order to account for out-of-plane failure modes, normally disregarded in past studies, linear static Finite Element analysis in 3D of prototype regular buildings is performed using a nonlinear biaxial failure criterion for masonry. More than 1100 analyses are carried out, so as to cover the practical range of the most important parameters, namely the number of storeys, percentage of side length in exterior walls taken up by openings, wall thickness, plan dimensions and number of interior walls, type of floor and pier height-to-length ratio. Results are presented in the form of damage and fragility curves. The fragility curves correspond well to the damage observed in masonry buildings after strong earthquakes and are in good agreement with other fragility curves in the literature. They confirm what is already known, namely that buildings with stiff floors or higher percentage of load-bearing walls are less vulnerable, and that large openings, taller storeys, larger number of storeys, higher wall slenderness and higher ratio of clear height to horizontal length of walls increase the vulnerability, but show also by how much.

Keywords: fragility curves; masonry buildings; seismic fragility; seismic vulnerability; unreinforced masonry buildings

1. Introduction

Masonry buildings, particularly old ones without seismic design, are an important fraction of the building stock in the world and are known to be highly vulnerable to earthquakes. Seismic fragility functions, which express the probability of exceeding specific damage states as a function of a seismic motion intensity measure, are essential for vulnerability studies and seismic scenarios of the damage in a town or region, should an earthquake occur. In order to provide a realistic estimate of the expected damage, fragility curves should be representative of the local structural typologies and properly account for the structural effects of the most important parameters.

Fragility curves for masonry buildings have been derived in the past from observed damage data, numerical analyses, or a combination of the two. Fragility curves based on data collected after major earthquakes in Greece were developed by Penelis *et al.* (2002) for one- and two-storey stone and brick masonry buildings and by Karababa and Pomonis (2011) for stone masonry buildings classified according to the period of construction. Colombi *et al.* (2008) used damage

*Corresponding author, Assistant Professor, E-mail: karmar@upatras.gr

data from six strong earthquakes in Italy since 1980 to produce fragility curves for low- and mid-rise masonry buildings. Using a similar database of recorded damage, Rota *et al.* (2008) derived fragility curves for a wider range of building classes, considering regularity in plan, type of floors and presence or not of tie-rods or beams. Damage from a series of shaking-table tests was used by Bothara *et al.* (2010) to derive fragility curves for two-storey brick masonry buildings with flexible floors. A weakness of empirical curves is that they cover few building typologies and earthquake intensities and are applicable only to areas with similar characteristics. To overcome this drawback, analytical methods have been used.

D'Ayala *et al.* (1997) performed limit state analysis assuming a number of in-plane and out-of-plane collapse mechanisms to produce vulnerability curves that were in good agreement with observed damage. Thanks to its simplicity, the capacity spectrum method is often used to develop fragility curves with a given standard deviation. To this end, semi-empirical expressions based on the geometry and material properties are used to define the bilinear capacity curve of a building deemed characteristic of a class, e.g., Cattari *et al.* (2004), Lagomarsino and Giovinazzi (2006), Lang and Bachman (2004). Pagnini *et al.* (2011) applied the same analysis method, but accounted in more detail for the uncertainties of the geometric and mechanical properties, earthquake characteristics and modelling. An advanced capacity spectrum method was employed by Frankie *et al.* (2013) along with a set of numerical and experimental capacity curves from literature. As an alternative to analytical expressions, pushover analysis of plane frame models has been performed to obtain the capacity curve needed in the framework of the capacity spectrum method, as in the hybrid method by Kappos *et al.* (2006), wherein numerical results are used to extrapolate observed damage data to values of the seismic intensity measure for which data is missing. Equivalent plane frames modelling of masonry buildings with stiff floors has been also employed in the framework of Monte Carlo simulations that account for uncertainty in the material properties used in the analysis, along with a large number of time-history analyses that integrate the variability of the earthquake input, e.g. Erberik (2008), Pasticier *et al.* (2008), Rota *et al.* (2010). Park *et al.* (2009) produced fragility curves for a two-storey masonry building using time-history analyses, where the piers and spandrels of the walls parallel to the seismic action were modelled by springs arranged in series or in parallel and single springs with a bilinear hysteresis rule simulated the walls normal to the seismic action. The out-of-plane response was critical and depended on the strength and boundary conditions of the walls normal to the direction of the earthquake.

In the present work, fragility curves for prototype, regular stone masonry buildings are developed based on analyses that consider both in-plane and out-of-plane response and behaviour; the latter was normally disregarded in past numerical studies. A very large number of analyses is carried out, in order to study and compare the effects of important geometric characteristics on seismic fragility. The analysis is in three-dimensions (3D), with finite elements (FE), but, owing to the large number of analysis runs necessary to cover the scope of the study, it is relatively simple: linear static, using a biaxial failure criterion in the stress domain to classify the damage. The results are validated against observed damage data and fragility curves from literature.

2. Building typologies

Irregularity in plan (e.g., Erberik 2008) or in elevation (e.g., Yi *et al.* 2006), result in concentration of damage and increased fragility. Prototype buildings, such as those considered in

this study, cannot cover possible irregularities, such as in the plan- and height-wise arrangement of openings, the location of interior bearing walls, set-backs, staircases, etc. Irregular structures are not covered in this study, which addresses the typical behaviour of regular, prototype buildings.

Prototype buildings are studied. They are built of modules, modified in plan and repeated in height. Two basic plans are used, with external dimensions 15.5×15.5 m and 22.0×22.0 m, as shown in Fig. 1. Both types of plan have no interior walls in one direction (x in Fig. 1); in the other direction (y in Fig. 1), the smaller-size buildings have one interior wall; the bigger ones have two. The first configuration is common in older unreinforced masonry (URM) buildings; the second layout enables to study the behaviour of buildings with long walls.

An important feature of masonry buildings from the point of view of seismic response is the stiffness of the floors and the roof. Reinforced concrete slabs, common in URM buildings of recent construction, act as rigid diaphragms. Older buildings have flexible floors, of wood or steel beams, and flexible roofs, of wood trusses. URM buildings with either stiff or flexible floors and roof are studied herein.

A further classification is based on the architectural features of the façade. In buildings where the exterior openings are mainly windows and spandrels have significant depth, the architecture places emphasis on the horizontal direction; the vertical one is emphasised in buildings with spandrels of reduced depth and openings (doors or windows) with a sill thinner than the walls, which acts as infill. In the present study, two types of buildings, depicted in Fig. 2, are analysed: in the first, the storey height is $h_{st} = 3.5$ m and the exterior walls have 1.5 m-tall windows; buildings of the second type have storey height $h_{st} = 4.5$ m and 3.0 m-high doors. This makes it possible to examine the effect of the wall pier height-to-length ratio, h/l , with h defined per Eurocode 8 (CEN 2004), as the greater clear height of the openings adjacent to the pier. Present-day seismic design codes impose limits on the h/l ratio; Eurocode 8 (CEN 2004) in particular requires that $h/l \leq 2.0$ in stone masonry buildings. The two typologies in Fig. 2 are found both in older and in new masonry buildings; therefore both are considered with stiff or flexible floors. Each of one of the prototype plans in Fig. 1 is combined with the two configurations and storey heights in Fig. 2.

The seismic vulnerability of URM buildings is commonly considered to increase with increasing total building height. In order to examine the effect of this parameter, buildings with two, four and six storeys are analysed.

The percentage of openings in the walls also affects the vulnerability of URM buildings. To investigate its effect, the length of openings in the exterior walls, whether windows or doors, is also taken as a variable. Pier length is taken as in Table 1, corresponding to percentage of side length of exterior walls taken up by openings ranging from 25% to 50%, as shown in the table.

Wall thickness is normally dictated by the number of storeys and local building tradition. Present-day seismic design codes often set a minimum value of the effective thickness, t_{ef} (equal to the wall thickness in non-cavity walls), and a maximum value of the ratio of wall effective height, h_{ef} , to t_{ef} , so as to limit the wall slenderness. The values of t_{ef} in Table 2 are considered in the present study: a value $t_{ef} = 0.60$ m is used as basis for two-storey URM masonry buildings, and increased by 25% or 50% to 0.75 m and 0.90 m. These values apply also to the two upper storeys of four- and six-storey buildings; the wall thickness is increased gradually at the lower storeys according to Table 2.

In order to study the effects of the parameters mentioned in the six paragraphs above, 216 prototype buildings are analysed, considering the following variables:

1. Plan per Fig. 1: 15.5×15.5 m and one interior wall, or 22.0×22.0 m and two interior walls.

2. Type of floor and roof: flexible or stiff.
3. Configuration in elevation per Fig. 2, with storey heights $h_{st} = 3.5$ m or $h_{st} = 4.5$ m.
4. Number of storeys: two, four and six.
5. Wall pier height-to-length ratio, h/l : 0.4 to 2.0.
6. Wall thickness, t_{ef} : 0.60 m to 1.45 m (see Table 2).

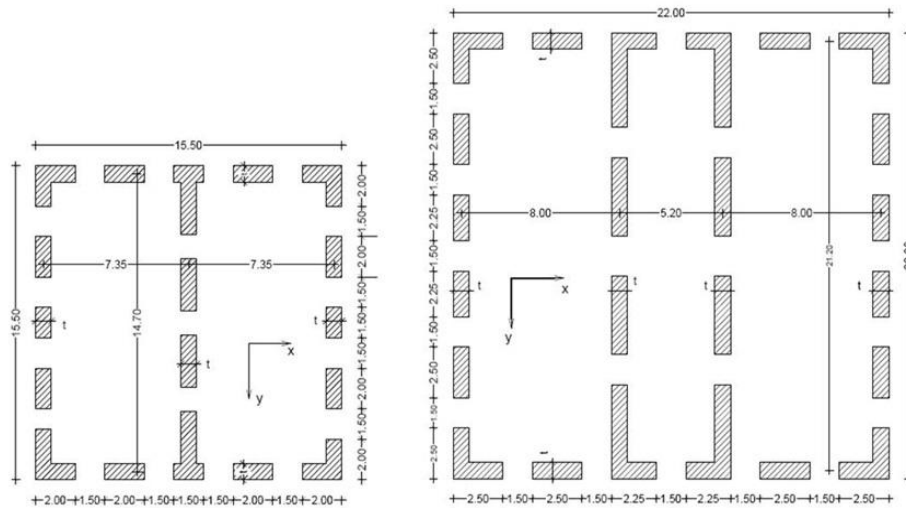


Fig. 1 Plan of buildings with one interior wall and 40% of exterior wall length taken up by openings (left) or two interior walls and 35% of exterior wall length taken up by openings (right)

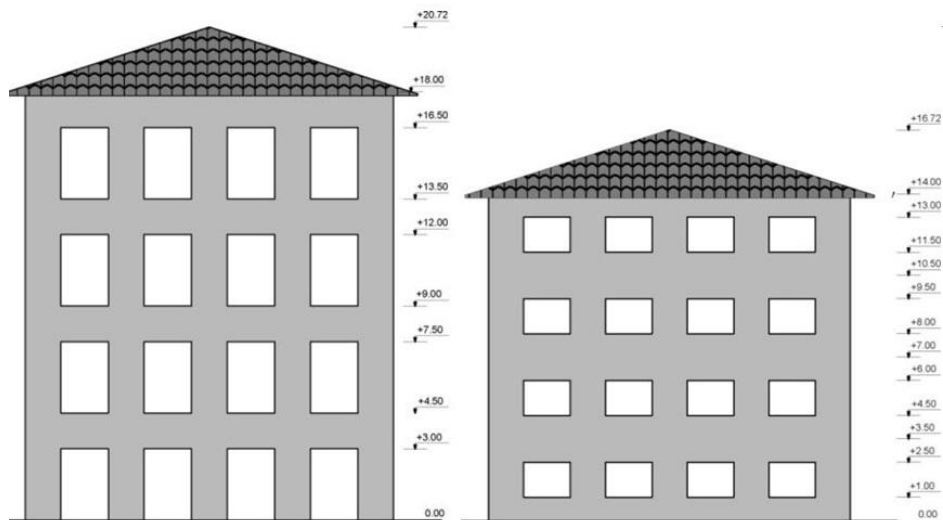


Fig. 2 Buildings with storey height $h_{st} = 4.5$ m and high h/l ratio (left) or $h_{st} = 3.5$ m and low h/l ratio (right)

Table 1 Length of wall piers, l , and resulting percentage of length of exterior walls taken by openings

	Buildings with one interior wall			Buildings with two interior walls		
Pier length, l (m)	1.5	2.0	2.5	2.0	2.5	3.0
Percentage of openings	50%	40%	25%	45%	35%	25%

Table 2 Wall thickness t_{ef} (m)

	Two-storey buildings			Four-storey buildings			Six-storey buildings		
Storeys 1-2	0.60	0.75	0.90	0.80	1.00	1.20	0.95	1.20	1.45
Storeys 3-4				0.60	0.75	0.90	0.80	1.00	1.20
Storeys 5-6							0.60	0.75	0.90

3. Damage grades

The five Damage Grades (DG) of the European Macroseismic Scale – EMS (Grünthal 1998) are used. The damage measure is taken as a function of the percentage and location of the surface area of the wall where one of the faces reaches a nonlinear biaxial failure criterion in terms of stresses, considering in-plane and out-of-plane response (biaxial normal forces and bending moments). As in the EMS damage grades, the damage measure is described using quantitative terms that are defined by narrowly overlapping percentage ranges. The damage measure is associated to the five damage grades as follows (the description of damage to structural elements per EMS given in parentheses):

1. Damage Grade 1 (hairline cracks in very few walls): no failure anywhere in the building, or at most minor cracking at very small areas at the top of the walls or the corners of the openings;
2. Damage Grade 2 (cracks in many walls): failure at small areas at the top of the walls, or at the corners of the building or of few openings;
3. Damage Grade 3 (large and extensive cracks in most walls): failure at medium-sized areas at the top of the walls or at the corners of the building or of openings, or over a large part of a single pier;
4. Damage Grade 4 (serious failure of walls): failure at larger areas at the top of the walls or at the corners of the building or of openings, or over large parts of several piers in a single wall;
5. Damage Grade 5 (total or near total collapse): failure over more than 50% of the total area of the walls or of a single wall.

4. Numerical analysis

Many past fragility studies of masonry buildings are based on analysis of equivalent frames that are not able to capture out-of-plane response. As an exception, D'Ayala *et al.* (1997) and Borzi *et al.* (2008) divided the walls in macro-elements and separately examined a number of plausible out-of-plane collapse mechanisms, while Park *et al.* (2009) simulated the out-of-plane response of the walls of a two-storey building by a bilinear hysteretic rule. In this work, each prototype building is analysed in 3D with Finite Elements (FE), and indeed using a fine discretization of each part of the wall. FEs are the only means to estimate the distribution, extent and even specific location of physical phenomena associated with damage and failure of the masonry material under the combined effects of in-plane and out-of-plane response. They also lend themselves to the use of

limit or failure criteria which are expressed in terms of masonry properties (e.g., strength), without arbitrarily adopting limit values, e.g., of interstorey drifts, which were developed in a another context and cannot be generalised to different situations.

Constitutive models for nonlinear analysis of URM walls are available for the 2D in-plane behaviour (see Magenes and Calvi 1997, Magenes 2010). Doherty *et al.* (2002) and Griffith *et al.* (2003) applied a tri-linear force-displacement model for the out-of-plane response of single walls. Two options are conceivable for nonlinear modelling of the generalised force-deformation behaviour of masonry walls under simultaneous in-plane and out-of-plane loading, for FE analysis in 3D:

a. The fundamental approach: a special purpose "shell" (: membrane-cum-plate) element for masonry, with discretisation of the wall thickness in layers, connected through the Bernoulli plane-sections hypothesis, and using in each layer a nonlinear biaxial stress-strain model for the masonry material (i.e., a generalisation of fibre elements from 1D elements to 2D plates);

b. A special purpose "shell" macro-element for masonry, with a nonlinear law between the three in-plane force resultants and the three moment resultants on one hand and the associated six deformation measures on the other; such an element may in principle be developed to fit the response from type-a modelling for typical load paths.

Numerical tools of either of these two types have not been developed and verified, at least for real-life practical applications with extent and scope as in this study. So, time-tested linear FE analysis is carried out instead, using a nonlinear biaxial failure criterion in terms of stresses. This is deemed sufficient for the purposes of the present work, as masonry is fairly brittle and cracking under biaxial stresses is the main feature of its nonlinear behaviour. This simplified modelling and analysis was found by Karantoni and Fardis (1992) to reproduce well the seismic damage in real buildings. At the expense of computational effort, this approach was also found to be superior to space-frame analysis in 2D or 3D, or even of truly nonlinear in-plane FE analysis in 2D, in predicting the distribution and severity of damage.

The walls are discretised into a fine mesh of "shell" elements with thickness that of the wall, for both in-plane behaviour and out-of-plane bending. Concrete slabs for the floors and the roof are modelled with FEs. Flexible floors of wood or steel beams in the x-direction, or flexible roofs of trusses supported on the four perimeter walls, are not modelled with their stiffness, as it is small compared to that of masonry walls. Moreover, their connection to the walls normally does not let them have a marked contribution to seismic resistance. The vertical reactions from the floors and the roof and the associated masses are lumped at the supporting wall nodes.

The nonlinear biaxial failure criterion by Karantoni *et al.* (1993) is used here to signal material failure. It is based on the assumption that under biaxial stresses, masonry cracks are normal to the principal tensile stress, if, at one of the two faces of the wall, a biaxial failure condition is reached, expressed in terms of the principal stresses σ_1, σ_2 (which account for shear and normal stresses referring to the horizontal and vertical directions). The model was obtained by adapting the well-known Ottosen (1977) four-parameter failure envelope for semi-brittle materials on the basis of a large number of biaxial tests on solid brick masonry wallettes, with the angle between the principal tensile stress and the masonry bed joints varying from 0° to 90° (Page 1983). The failure envelope for idealised isotropic masonry under triaxial stress conditions is:

$$\alpha \frac{J_2}{f_{wc}^2} + \lambda \frac{\sqrt{J_2}}{f_{wc}} + \beta \frac{I_1}{f_{wc}} = 1 \quad (1)$$

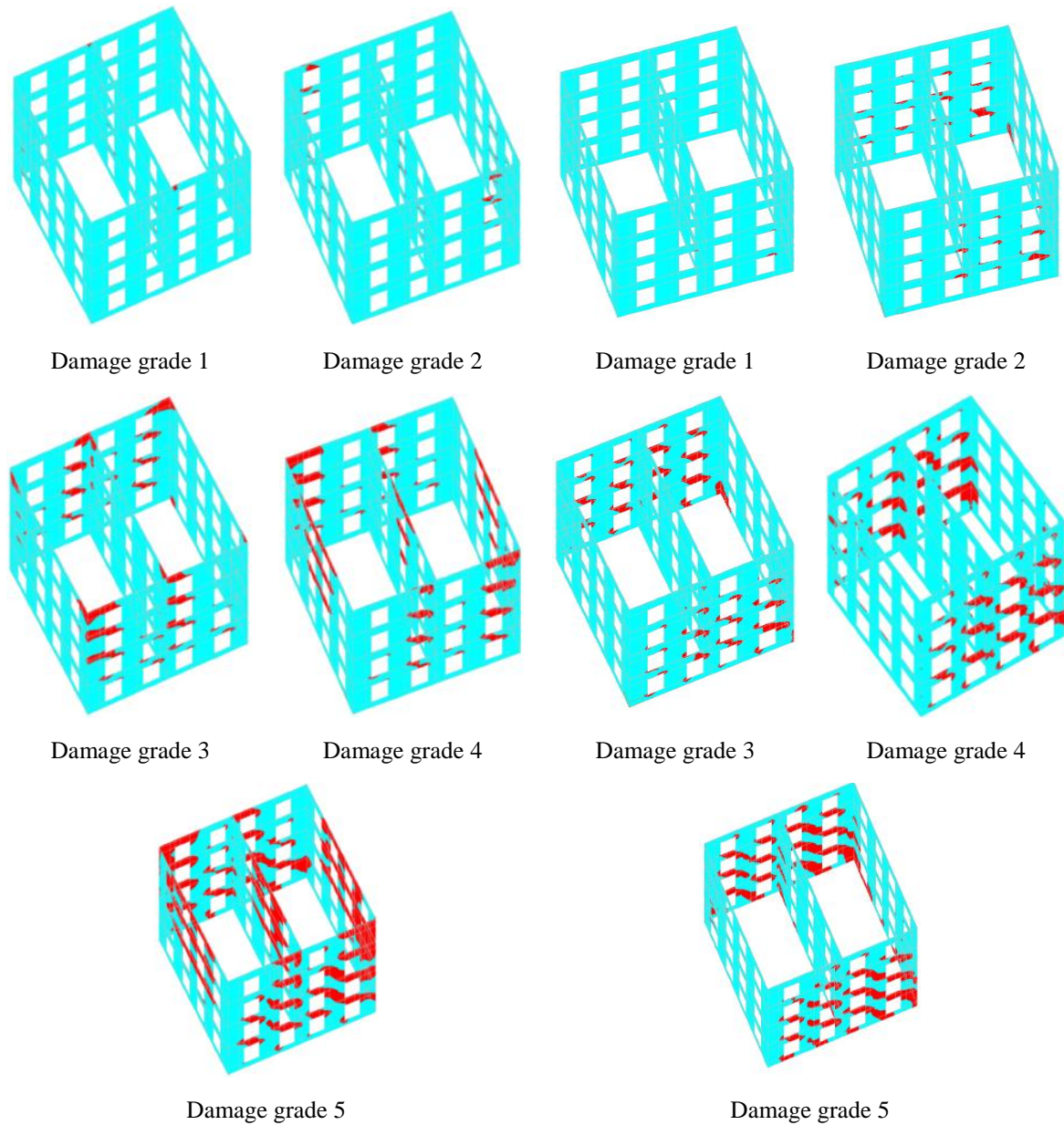


Fig. 3 Results of FE analyses of four-storey building with flexible (left) or stiff (right) floors

where I_1 is the first stress invariant, J_2 the second deviatoric stress invariant and f_{wc} the masonry compressive strength. Parameter λ depends on the inclination of the octahedral plane, θ :

$$\lambda = c_1 \cos \frac{\cos^{-1}(c_2 \cos 3\theta)}{3}, \text{ if } \cos 3\theta \geq 0 \quad (2)$$

$$\lambda = c_1 \cos \frac{\pi - \cos^{-1}(-c_2 \cos 3\vartheta)}{3}, \text{ if } \cos 3\vartheta \leq 0 \quad (3)$$

where:

$$\cos 3\vartheta = \frac{3\sqrt{3}J_3}{2J_2^{3/2}} \quad (4)$$

with J_3 the third deviatoric stress invariant. Note that $\theta = 60^\circ$ for uniaxial compression and $\theta = 0^\circ$ for uniaxial tension or biaxial compression. Because of the isotropic behaviour of uncoursed rubble stone masonry, the values of principal stresses at failure reported by Page (1983) were averaged, for all angles between the principal tensile stress and the masonry bed joints. The values of the parameters α , β , c_1 and c_2 were fitted to the test data, as:

$$\alpha = 0.665, \beta = 3.84, c_1 = 13.8, c_2 = 0.959 \quad (5)$$

The analyses are carried out with tensile strength of masonry $f_{wt} = 0.085f_{wc}$, where f_{wc} is the compressive strength, considered with a basis value of $f_{wc} = 3.5$ MPa and varied in the framework of parametric studies. The modulus of elasticity of uncracked masonry is taken as $E = 1000f_{wc}$ (CEN 2005); it is reduced in the analysis by 50% to account for distributed minor cracking before failure, as in most present day seismic design codes. The vertical loads on the model comprise the self-weight of masonry for a specific weight of $\gamma = 22$ kN/m³. The self-weight of floors and roof and a quasi-permanent live load on floors amount to 6 kN/m².

The analysis is static under lateral forces with an inverted triangular distribution, as appropriate for response dominated by the first mode. In line with present day seismic design codes, stresses due to the two horizontal components of the seismic action along axes x (normal to the interior walls) and y (parallel to them), E_x and E_y , are combined as “ $E_x + 0.3E_y$ ” and “ $0.3E_x + E_y$ ”.

The lateral forces are taken proportional to the mass they are applied to, times the vertical distance from the base of the building, times an effective spectral acceleration, $S_{a,eff}$. As for buildings of the type considered here the fundamental period is in the constant-acceleration plateau of the response spectrum, it may be assumed that:

$$S_{a,eff} = 2.5a_g/q(DG) \quad (6)$$

In Eq. (6) a_g is the peak ground acceleration (PGA) at the base of the building and $q(DG)$ an effective force reduction (or “behaviour”) factor reflecting the different levels of damping and damage associated with each Damage Grade.

More specifically:

- For Damage Grade 1, corresponding to almost elastic response:

$$q(1) = 1 \quad (7)$$

- For Damage Grade 5:

– For buildings with stiff floors: a basic value $q_{Ro}(5) = 2$ is assumed (in Eurocode 8 the recommended value of this factor for URM buildings designed for seismic resistance is from 1.5 to 2.5); $q_{Ro}(5)$ is subsequently multiplied by an overstrength factor $\alpha_u/\alpha_1 = 2$, as proposed by Magenes (2010) to account for the actual behaviour of masonry structures after the first structural element fails, resulting in:

$$q_R(5) = 4 \quad (8a)$$

– Buildings with flexible floors are expected to reach Damage Grade 5 with less energy dissipation and lower ductility; for this reason a lower value of the effective behaviour factor is appropriate:

$$q_F(5) = 3 \quad (8b)$$

• Linear interpolation between Eqs. (7) and (8) is used for intermediate Damage Grades.

Note that Eqs. (8) are based on educated assumptions. Should another assumption seem more plausible, it may be used instead, affecting only the translation of a_g to $S_{a,eff}$ and vice-versa via Eq. (6).

Indicative results of the FE analyses for a four-storey building with flexible or stiff floors and for the main component of the seismic action parallel to y (i.e., normal to the interior walls) are shown in Fig. 3 for the five Damage Grades. Dark (in red) are shown the areas where the failure criterion, Eqs. (1)-(5), is exceeded. Different damage patterns are observed for the two types of floors. Owing to the poor connection between the walls, the building with flexible floors suffers damage at the four corners and the intersections of interior and exterior walls. The higher Damage Grades are characterised by out-of-plane damage at the upper part of walls having large spacing between cross-walls. By contrast, the building with stiff floors presents a damage pattern with predominantly in-plane failures, concentrated at the lower storeys.

5. Generation of fragility curves

Linear static analyses of each building model were carried out per Section 4, under values of $S_{a,eff}$ from 0.05g to 0.20g at increments of 0.05g and at increments of 0.10g until 0.60g, aiming to reach all Damage Grades in each building. However, for some two-storey buildings with stiff floors the highest Damage Grades are not observed even at $S_{a,eff} = 0.60g$. More than 1100 analyses were performed in total, so that almost all of the 216 buildings reach the five Damage Grades for both combinations of the horizontal components of the seismic action. For each analysis, a Damage Grade is assigned to the building after examining the location and surface area where the failure criterion of Eqs. (1)-(5) is exceeded at either the inner or the outer face of the walls. The fragility may be expressed using as Intensity Measure (IM) either $S_{a,eff}$ directly (in which case they are independent of the assumptions behind Eqs. (8)), or - inverting Eq. (6) for a_g - the corresponding PGA value at the base of the building, a_g .

Fragility curves were developed for building classes described by three parameters, namely the number of storeys (two, four and six), the type of floors (flexible or stiff) and the aspect ratio of openings (h/l higher or lower than 1.0). For each class and value of peak ground acceleration, the number of buildings that reach a Damage Grade is counted and the corresponding probability of exceeding the Damage Grade calculated as the fraction of buildings which have reached that Grade to the total number. Assuming a lognormal distribution, a continuous curve was fitted to the discrete data points and its median, μ , and standard deviation, β' , are calculated. In Fig. 4 the lognormal fragility curves for four-storey buildings with stiff floors and high h/l ratio are compared to the empirical data points. The Kolmogorov-Smirnov statistic, D_{max} , and the critical value for 5% significance level, $D_{crit,5\%}$, are also reported in Fig. 4. Goodness-of-fit was verified for all cases according to the Kolmogorov-Smirnov method for 5% significance level.

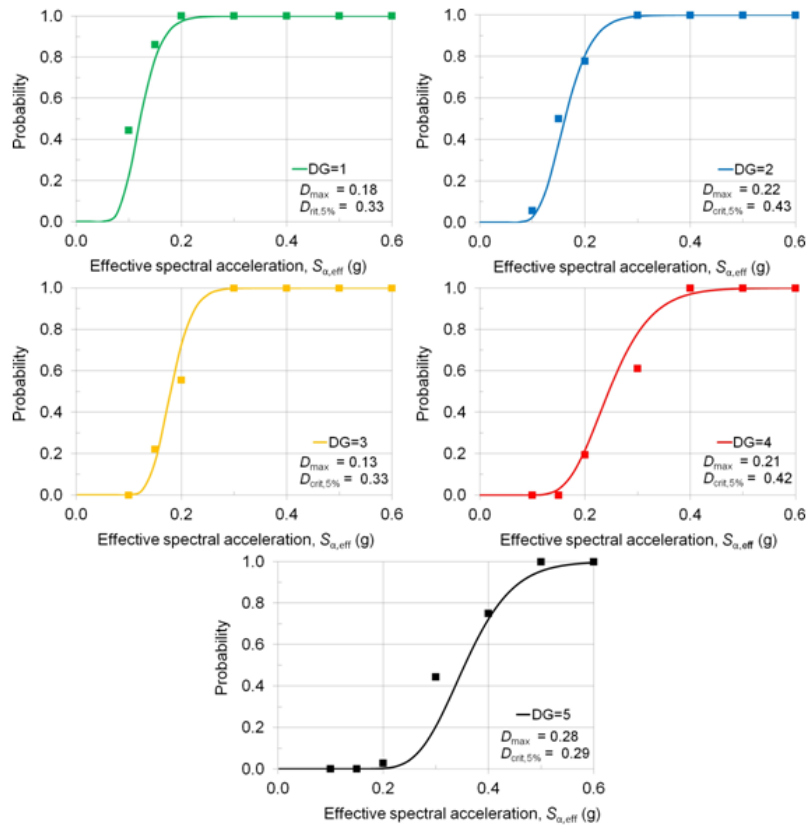


Fig. 4 Comparison of lognormal (continuous line) fragility curves to empirical data points for four-storey buildings with stiff floors and high h/l ratio

Table 3 Median, μ , and standard deviation, β , of fragility curves of classes of stone masonry buildings for Damage Grades DG1 to DG5 (median in terms of a_g or $S_{a,eff}$ times $3.5/f_{wc}$ (MPa))

Floor type	h/l	Two-storey buildings					Four-storey buildings					Six-storey buildings					
		DG1	DG2	DG3	DG4	DG5	DG1	DG2	DG3	DG4	DG5	DG1	DG2	DG3	DG4	DG5	
Flexible	>1.0	$\mu(a_g)$	0.03	0.07	0.16	0.24	0.37	0.02	0.05	0.08	0.14	0.25	0.03	0.04	0.06	0.10	0.18
		$\mu(S_{a,eff})$	0.08	0.12	0.20	0.24	0.31	0.05	0.08	0.10	0.14	0.21	0.07	0.08	0.09	0.10	0.15
		β	0.75	0.65	0.72	0.78	0.70	0.67	0.68	0.73	0.71	0.75	0.67	0.67	0.69	0.69	0.69
	<1.0	$\mu(a_g)$	0.05	0.10	0.17	0.31	0.48	0.03	0.05	0.11	0.18	0.26	0.03	0.06	0.09	0.15	0.27
		$\mu(S_{a,eff})$	0.13	0.17	0.21	0.31	0.40	0.08	0.09	0.14	0.18	0.22	0.08	0.10	0.11	0.15	0.23
		β	0.65	0.67	0.69	0.76	0.66	0.73	0.69	0.74	0.79	0.70	0.66	0.73	0.74	0.74	0.70
Stiff	>1.0	$\mu(a_g)$	0.07	0.18	0.33	0.54	0.73	0.05	0.11	0.18	0.32	0.57	0.03	0.09	0.13	0.23	0.42
		$\mu(S_{a,eff})$	0.18	0.26	0.33	0.42	0.46	0.13	0.16	0.18	0.25	0.36	0.08	0.12	0.13	0.18	0.26
		β	0.63	0.65	0.66	0.65	0.62	0.65	0.65	0.63	0.65	0.63	0.74	0.65	0.65	0.63	0.65
	<1.0	$\mu(a_g)$	0.10	0.28	0.45	0.65	0.90	0.07	0.15	0.27	0.44	0.69	0.05	0.12	0.19	0.30	0.45
		$\mu(S_{a,eff})$	0.25	0.40	0.45	0.50	0.56	0.18	0.21	0.27	0.34	0.43	0.13	0.17	0.19	0.23	0.28
		β	0.65	0.64	0.62	0.62	0.61	0.64	0.66	0.65	0.63	0.64	0.65	0.64	0.62	0.67	0.64

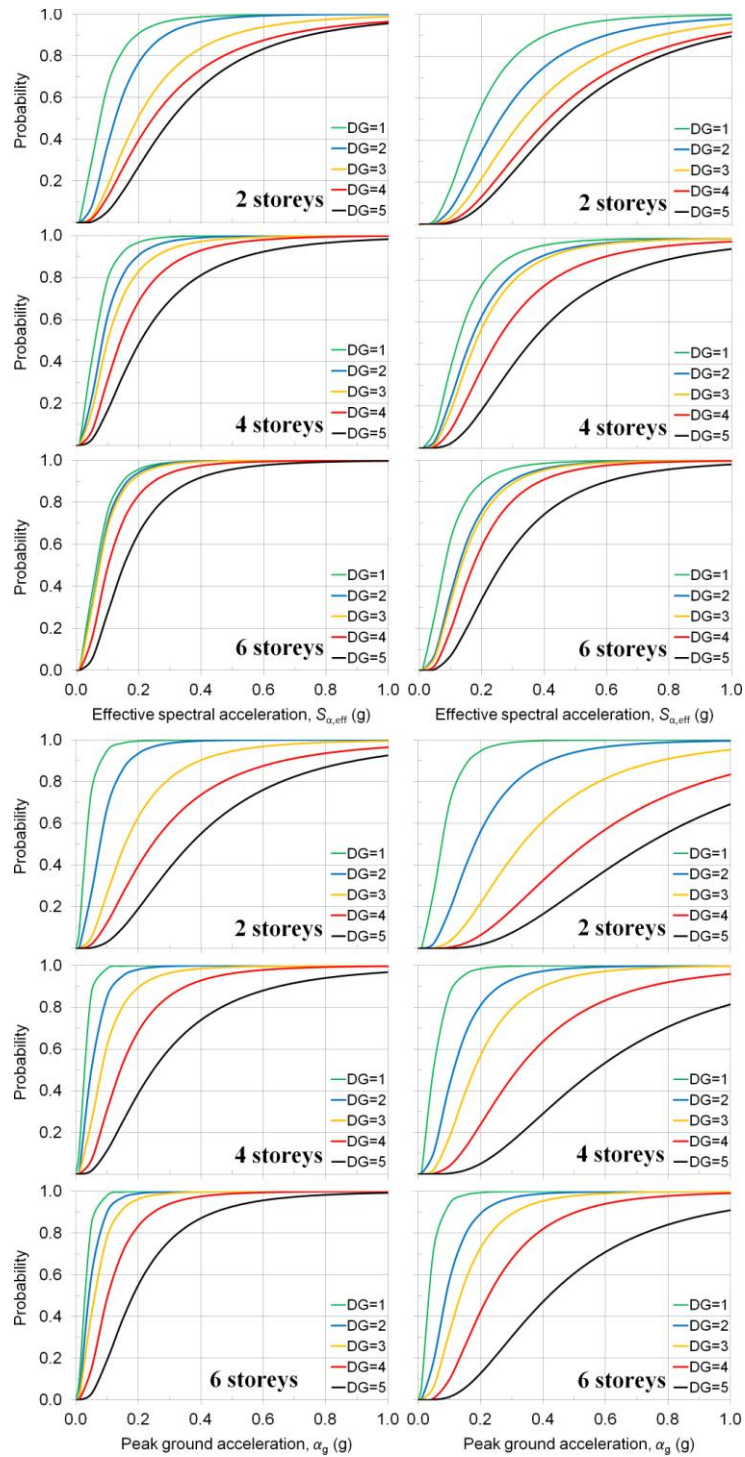


Fig. 5 Fragility curves of two-storey, four-storey and six-storey buildings with flexible (left) or stiff floors (right) and $h/l \geq 1.0$ (for $f_{wc} \neq 3.5$ MPa, horizontal axis is entered with IM multiplied by $3.5/f_{wc}$ (MPa))

The standard deviation β' reflects variations in the geometry of the building (wall thickness, plan dimensions, number of interior walls, percentage of side length in exterior walls taken up by openings) within the class and the effect of the direction of the principal horizontal seismic action component. In order to account for other sources of uncertainty, e.g. the characteristics of the seismic input, the variability of resistance, etc., the standard deviation calculated on the basis of the FE analyses is combined with the value 0.6 commonly assumed in fragility analysis, i.e. as:

$$\beta = \sqrt{(\beta')^2 + 0.6^2} \quad (9)$$

The so determined values of μ and β for each building class are presented in Table 3. Although the approximation in Eq. (9) was used, the resulting values are similar to those computed by Erberik (2008) on the basis of nonlinear time-history analyses with 50 records – see comparison of the fragility curves in Section 8.2 – and close to $\beta = 0.64$, suggested by FEMA (2010) for all damage grades and building types when a_g is the seismic intensity measure.

Examples of fragility curves developed according to the procedure above are shown in Fig. 5 for buildings with two, four and six storeys and stiff or flexible floors and in Figs. 6-9 for other combinations of parameters.

A basis value of the masonry compressive strength $f_{wc} = 3.5$ MPa was used in the bulk of the analyses. Parametric studies showed that the decrease in Damage Grade with increasing masonry strength may be approximated by taking the value of the acting $S_{a,eff}$ or a_g as inversely proportional to f_{wc} . Then, the results may be approximately adjusted to other values of masonry strength, by entering the horizontal axis of Figs. 5-9 with the value of $S_{a,eff}$ or a_g multiplied by $3.5/f_{wc}$ (MPa).

If different assumptions lead to values of $q(5)$ different than those in Eqs. (8), then, the resulting value of $q(DG)$, denoted here as $q'(DG)$, should be used in Eq. (6) alongside the parts of Figs. 5-9 expressed in terms of $S_{a,eff}$ to express the fragility curves as a function of a_g . The outcome would be equivalent to entering the horizontal axis of the parts of Figs. 5-9 expressed in terms of a_g , with the value of a_g multiplied by $q'(DG)/q(DG)$.

In Section 6 the fragility curves are used to study the parameters that affect the seismic vulnerability of URM buildings, while in Section 8 it is shown that they are consistent with the damage suffered by stone masonry buildings after strong earthquakes.

6. Effect of building geometry on seismic fragility

The fragility curves developed in this study show by how much the buildings with flexible floors are always more vulnerable than those with stiff floors (compare left to right columns in Figs. 5-9 and also the μ -values in Table 3). The improvement in performance of buildings with stiff floors is also evident from the ample margins between Damage Grades, whereas a small increment of the Intensity Measure is sufficient to lead buildings with flexible floors to a higher Damage Grade. Fig. 5 shows also by how much taller buildings are more vulnerable. Indicatively, the probability of exceeding Damage Grade 4 for $a_g = 0.3g$ ($S_{a,eff} = 0.3g$) is 60%, 85% and 94% for buildings with flexible floors and two, four, or six storeys, respectively. Note also that six-storey buildings with stiff floors are comparable in terms of fragility to two-storey buildings with flexible floors – respectively 68% and 60% probability of exceeding Damage Grade 4 for $a_g = 0.3g$.

The fragility curves in Fig. 6 show by how much buildings with low h/l -ratio are more vulnerable than those with high h/l values. By way of example, for buildings with stiff floors the

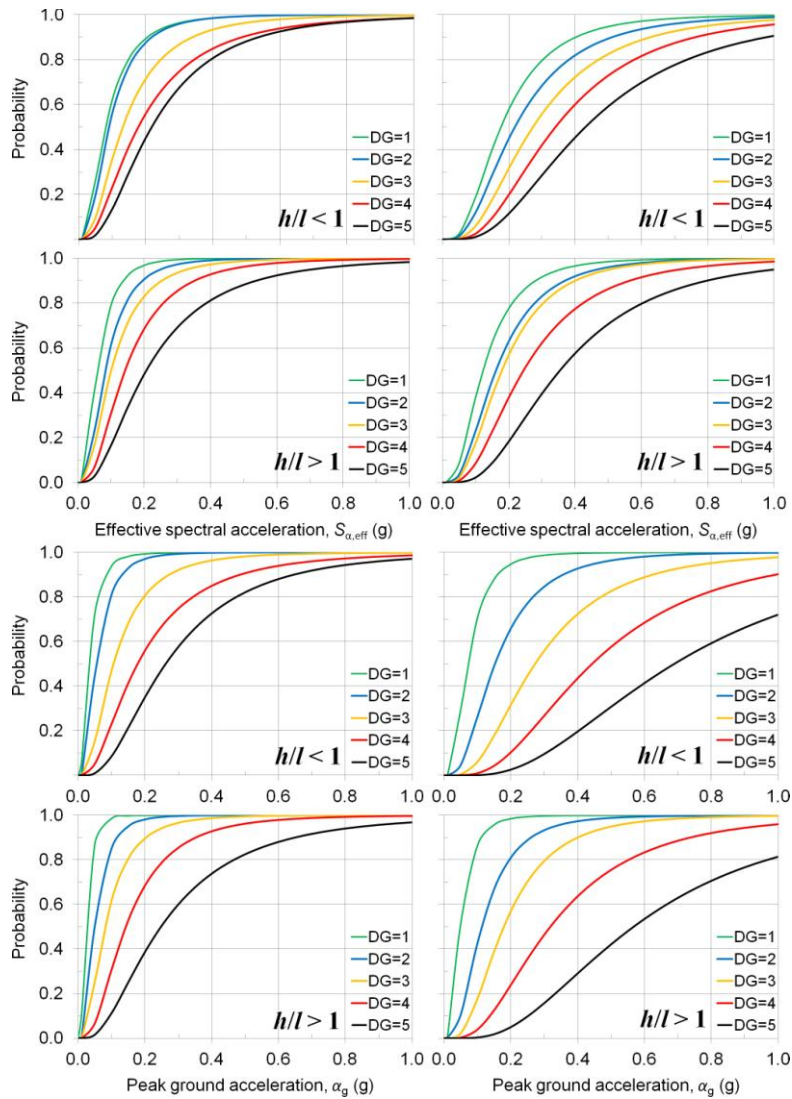


Fig. 6 Fragility curves of four-storey buildings with flexible (left) or stiff (right) floors and low or high h/l -ratio (for $f_{wc} \neq 3.5$ MPa, horizontal axis is entered with IM multiplied by $3.5/f_{wc}$ (MPa))

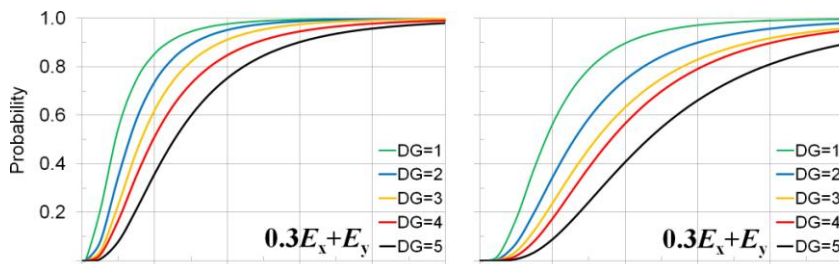


Fig. 7 Continued

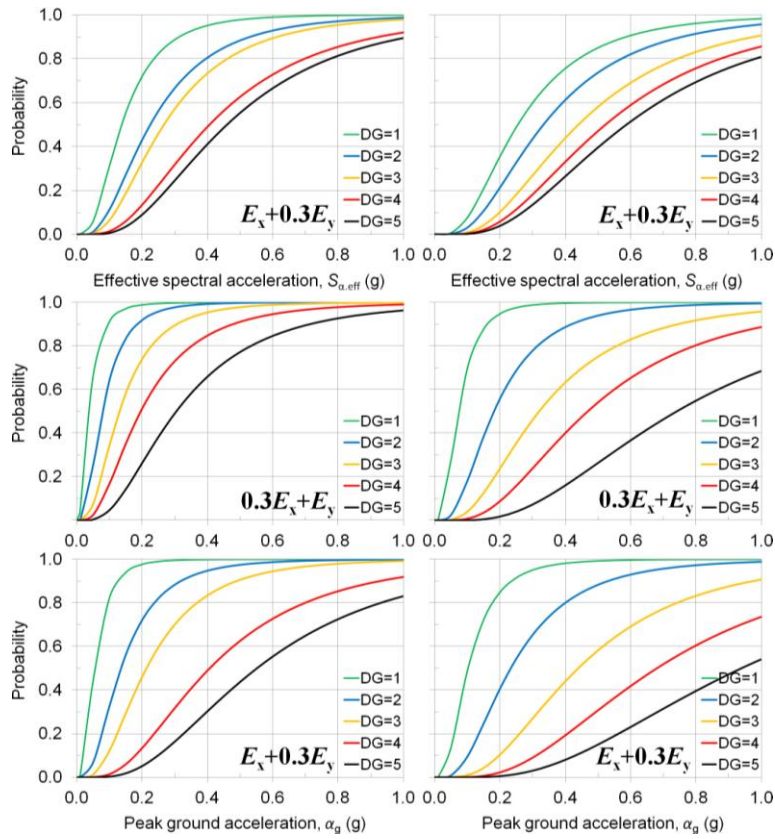


Fig. 7 Fragility curves of two-storey buildings with flexible (left) or stiff floors (right), for the main seismic action component normal or parallel to the interior walls (for $f_{wc} \neq 3.5$ MPa, horizontal axis is entered with IM multiplied by $3.5/f_{wc}$ (MPa))

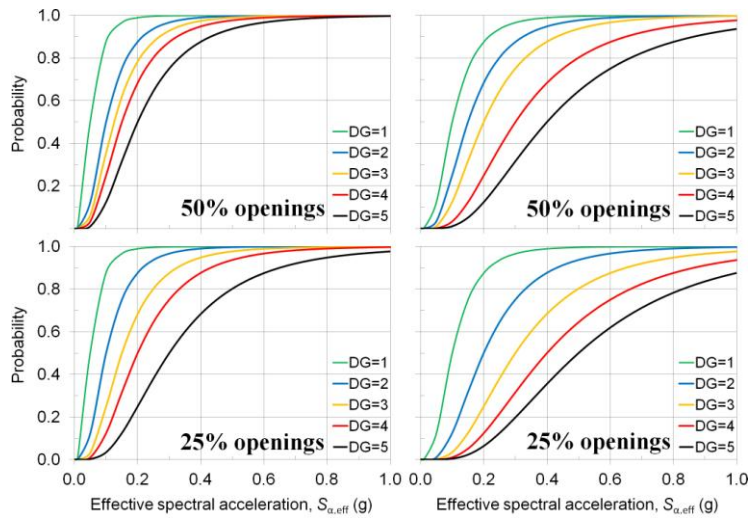


Fig. 8 Continued

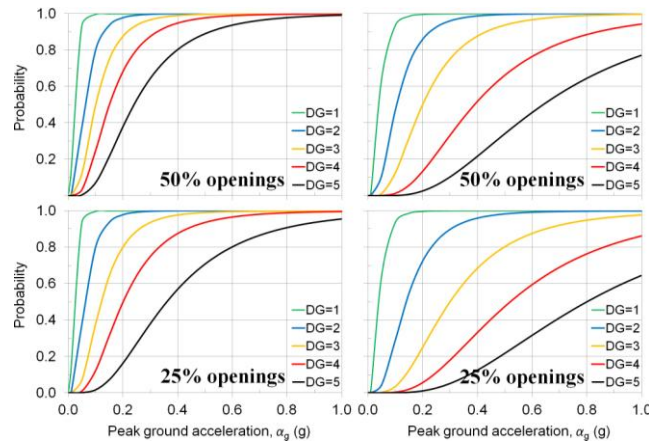


Fig. 8 Fragility curves of four-storey buildings with $h_{st} = 4.5$ m and $t_{ef} = 1.0$ m at the ground storey, flexible (left) or stiff floors (right), 50% or 25% openings in the perimeter walls, for the main seismic action component parallel to the two interior walls (for $f_{wc} \neq 3.5$ MPa, horizontal axis is entered with IM multiplied by $3.5/f_{wc}$ (MPa))

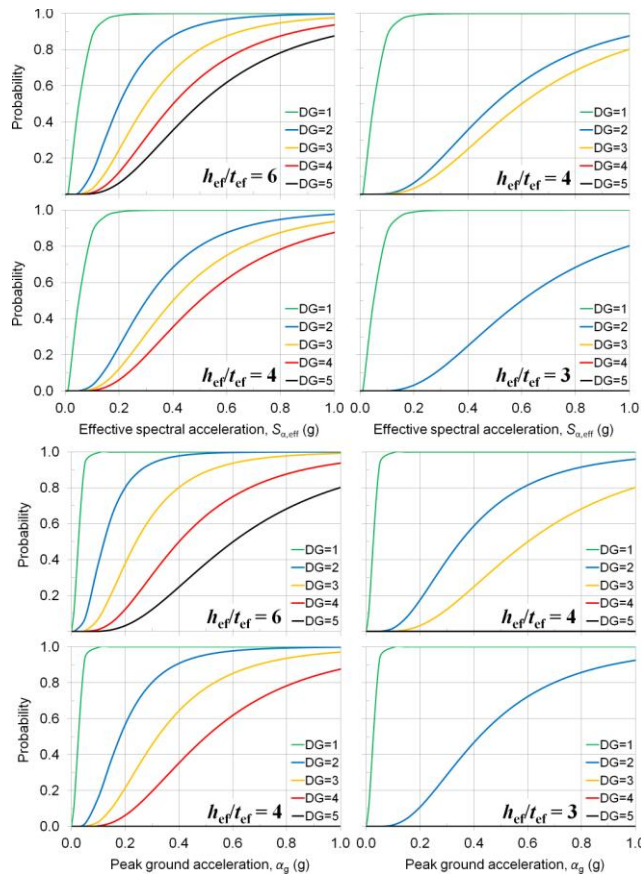


Fig. 9 Fragility curves of two-storey buildings with $h_{st} = 3.5$ m, flexible (left) or stiff floors (right), $t_{ef} = 0.6$ m or $t_{ef} = 0.9$ m at the ground storey, for the main seismic action component parallel to the interior wall (for $f_{wc} \neq 3.5$ MPa, horizontal axis is entered with IM multiplied by $3.5/f_{wc}$ (MPa))

probability of exceeding Damage Grade 4 at $a_g = 0.3g$ ($S_{a,eff} = 0.23g$) is 27% for $h/l < 1$ and rises to 46% for $h/l > 1$. The wall pier height-to-length ratio appears to affect the higher Damage Grades the most among all parameters considered.

Fig. 7 demonstrates the importance of interior load-bearing walls, not only for the sharing of the in-plane forces but also in bracing the orthogonal walls against out-of-plane damage. Their effect is more pronounced when the floors are flexible. When subjected to the combination $E_x + 0.3E_y$, i.e. for the main component of the seismic action normal to the walls with large spacing between bracing walls, buildings with flexible floors exhibit a large increase in damage for a small increase in Intensity Measure. In contrast, whereas there is a larger margin between Damage Grades for the combination $0.3E_x + E_y$, i.e. for the main component of the seismic action normal to the walls with shorter span, which does not activate the out-of-plane response. Such difference is much less pronounced in the case of stiff floors, where the interior walls contribute mainly in resisting the in-plane seismic action. In buildings with flexible floors the probability of exceeding Damage Grade 4 at $a_g = 0.3g$ ($S_{a,eff} = 0.3g$) reduces from 73% in the y-direction to 32% in the x-direction; for buildings with stiff floors it decreases from 24% to 9%, respectively.

The effect of the percentage of openings in the perimeter walls is shown in Fig. 8, where the fragility curves refer to specific four-storey buildings with high h/l -ratio ($h_{st} = 4.5$ m), wall thickness $t_{ef} = 1.0$ m at the two lower storeys and the main component of the seismic action parallel to the two interior walls (i.e. for the combination $0.3E_x + E_y$). The median value of the fragility is obtained from the FE analysis of the specific buildings; the standard deviation is conventionally taken as $\beta = 0.6$ for all buildings and Damage Grades. Fig. 8 shows by how much the vulnerability increases in buildings with more openings. For instance, the probability of exceeding Damage Grade 4 in buildings with stiff floors for $a_g = 0.3g$ ($S_{a,eff} = 0.23g$) is 33% when the openings take up half of the length of exterior walls, reducing to 18% if the length of openings is 25% of the total of exterior walls. The corresponding percentages for buildings with flexible floors are 88% and 75%. Witness that the percentage of openings affects mainly the higher Damage Grades in buildings with flexible floors, where the out-of-plane response is critical. In contrast, it affects all Damage Grades in buildings with stiff floors, as the in-plane response, which depends on the percentage of openings, is dominant. Similar observations hold for buildings with two or six storeys.

Fragility curves for individual two-storey buildings with low h/l -ratio ($h_{st} = 3.5$ m) and one interior wall are plotted in Fig. 9, so as to illustrate the effect of wall slenderness ratio, h_{ef}/t_{ef} . The effective height, h_{ef} , is taken here to depend on the relative stiffness of the elements connected to the wall according to Eurocode 6 (CEN 2005), which gives h_{ef} in a wall with free vertical edges (in this case, between openings) as $h_{ef} = h_{st}$ for flexible and $h_{ef} = 0.75h_{st}$ for stiff floors (h_{st} is the storey height). Similar to that of the percentage of openings, the effect of h_{ef}/t_{ef} is more marked on buildings with stiff floors, for which the probability of exceeding Damage Grade 2 for $a_g = 0.4g$ ($S_{a,eff} = 0.57g$) drops from 59% to 47%, whereas for flexible floors it changes from 98% to 91%. The curves for the highest Damage Grades are not shown in Fig. 9, as for those specific buildings they were not attained for the maximum value $S_{a,eff} = 0.6g$ considered in the FE analysis. This is confirmed by field observations that regular in plan and in elevation low-rise masonry buildings with stiff floors suffer only moderate damage even under strong earthquakes.

7. Damage curves

The results of FE analyses are used below to study the effect of the most important geometric parameters on the vulnerability of URM buildings through damage curves that present the damage state of a building as a function of spectral acceleration, $S_{a,eff}$.

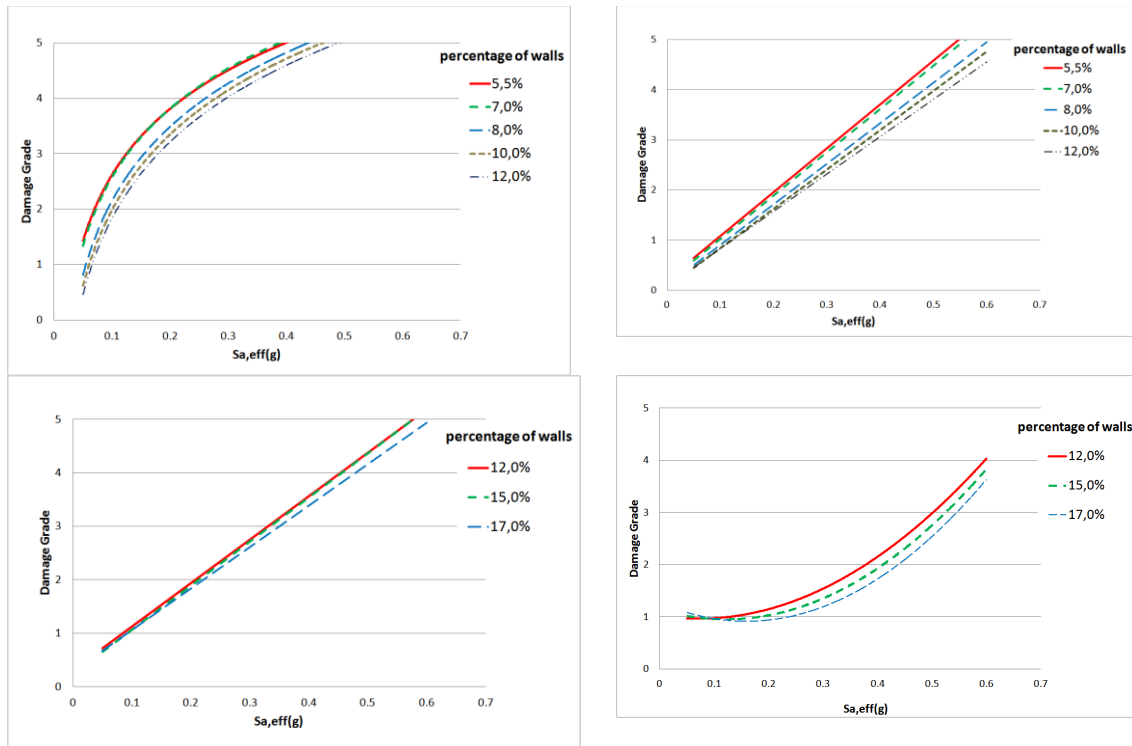


Fig. 10 Effect of the percentage of wall area on damage curves of two-storey buildings with flexible (left) or stiff (right) floors, for the main seismic action component normal (top) or parallel to the interior walls (bottom)

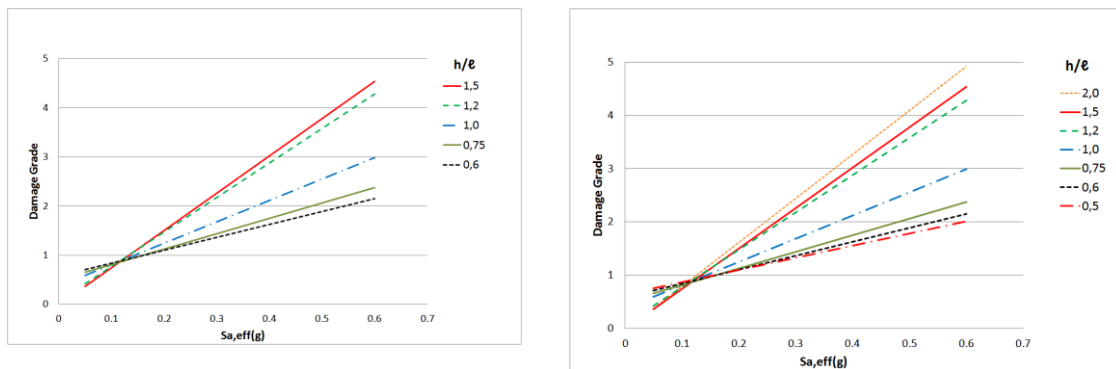


Fig. 11 Effect of h/l ratio on damage curves of two-storey buildings with flexible (left) or stiff (right) floors, for main seismic action component parallel to the interior walls

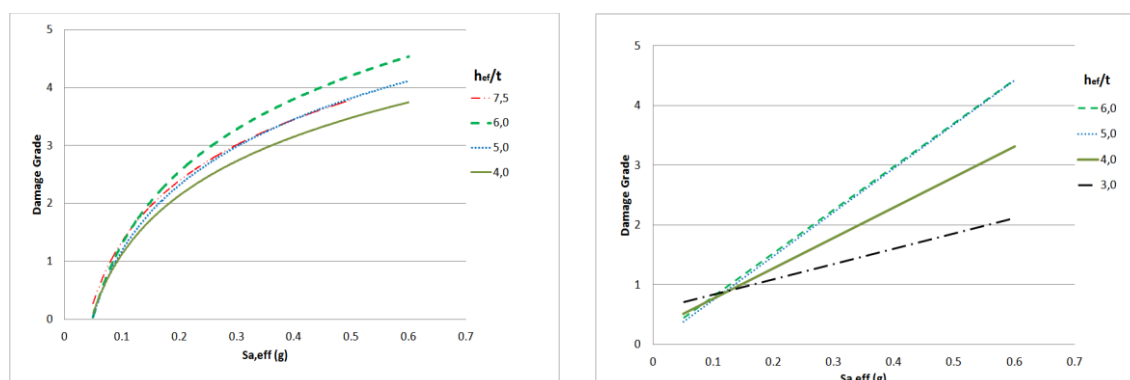


Fig. 12 Effect of wall slenderness on damage curves of two-storey buildings with flexible (left) or stiff (right) floors, for main seismic action component parallel to the interior walls

Fig. 10 depicts damage curves for two-storey buildings with stiff (right side) or flexible (left side) floors and different values of the percentage of the total ground floor area taken up by the walls parallel to the main seismic action. The following comments can be made:

- For buildings with flexible floors and for the main component of the seismic action normal to the interior walls (Fig. 10 top left) the out-of-plane response of the walls with long span is dominant. The Damage Grade may be approximated by a logarithmic function of the effective spectral acceleration, $S_{a,eff}$. However, percentage of wall area does not have a systematic effect on vulnerability, at least within the range of wall areas considered.

- For the main component of the seismic action parallel to the interior walls in buildings with flexible floors (Fig. 10 bottom left) the span of walls for out-of-plane flexure is shorter. There is a linear relation between Damage Grade and $S_{a,eff}$, but Damage Grade is independent of the percentage of wall area.

- By contrast, the vulnerability of buildings with stiff floors is influenced by the percentage of wall area. Witness in Fig. 10 right top and bottom the gradual reduction of vulnerability for higher percentage of wall area in buildings with stiff floors and the main component of the seismic action either parallel or normal to the interior walls. However, for seismic action parallel to the interior walls, damage is affected by the percentage of wall area only for high levels of $S_{a,eff}$; at lower levels all three curves are horizontal, i.e. independent of the percentage of wall area, there is no damage until $S_{a,eff}$ exceeds 0.20g.

The wall height-to-length, h/l , ratio and the wall slenderness, h_{ef}/t_{ef} , affect more the vulnerability in buildings with stiff floors than in those with flexible floors, as shown in Figs. 11 and 12. In Fig. 11, two distinct groups of buildings are identified: those with $h/l > 1$ are much more vulnerable compared to those with low height-to-length ratio. Moreover, buildings with stiff floors and low h/l ratio exhibit a much smaller rate of increase in Damage Grade with $S_{a,eff}$, compared to the other URM classes. The results in Fig. 12 show by how much buildings with higher h_{ef}/t_{ef} ratio are more vulnerable to earthquakes. As observed previously for the percentage of openings and the h/l ratio, the effect of slenderness ratio on the vulnerability is less significant in buildings with flexible floors than in those with stiff. Four- and six-storey buildings, not shown here for brevity, exhibit similar behaviour and even more pronounced out-of-plane effects.

8. Validation of fragility curves

8.1 Comparison to observed damage

The fragility curves developed according to the procedure described in Sections 3 to 5 are first compared to damage data collected after the 1995 Aegion (Greece) earthquake. During this $M_s = 6.2$ event, PGA values as high as 0.54g were recorded. Buildings suffered heavy damage, owing also to significant topographic amplification of the ground motion along the crest of a ridge. Following the earthquake, a team from the University of Patras recorded the damage of the building stock throughout the town. Regarding masonry buildings, information was collected about the location, number of storeys, material (stone, brick, adobe or mixed), and type of floor and roof (stiff or flexible). Data were collected for 857 URM buildings, among which 342 had one storey, 513 had two storeys and only two had three. Damage was assessed according to the damage scale described in Section 3. The location of the buildings and the Damage Grades are shown in Fig. 13. Throughout the town, 37% and 59% of one- and two-storey buildings, respectively, and all three-storey ones, showed some degree of damage (Karantoni and Fardis 2005). More extensive damage was observed in the historic centre, indicated by the thick line in Fig. 13, where 53% of one-storey and 71% of two-storey buildings were damaged. Out of the 376 masonry buildings in the historic centre, approximately one third had one storey; the rest had two storeys. Most URM buildings in the historic centre were of stone masonry with wooden floors and roofs and $h/l > 1$.

Bouckovalas *et al.* (1999) estimated the a_g -value at nine borehole locations within the city from the results of one- and two-dimensional soil-response analyses that accounted for topography effects and soil stratigraphy. The recorded damage data and the a_g -values at seven locations within the historic centre are used to validate the numerical fragility curves developed according to the procedure in Sections 3-5. The historic centre was divided in seven districts around the boreholes and the percentage of URM buildings that reached a given Damage Grade was calculated from the damage observed in each district. The discrete values of the probability of exceeding the five Damage Grades are plotted in Fig. 14 against the estimated PGA, together with the continuous fragility curves from FE analyses for two-storey buildings with flexible floors and $h/l > 1$, as in the

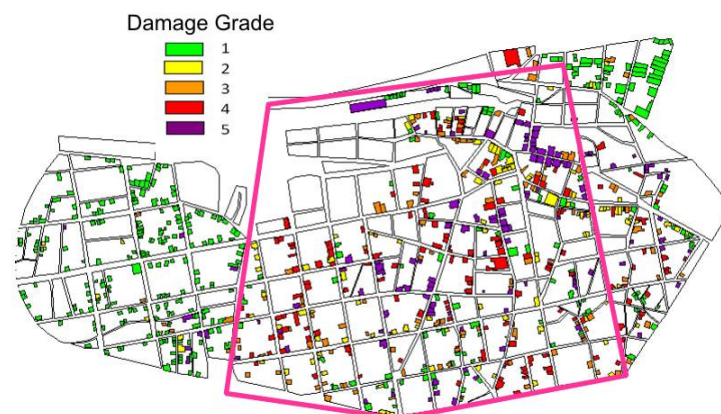


Fig. 13 Distribution of damaged URM buildings in the town centre of Aegion (GR)

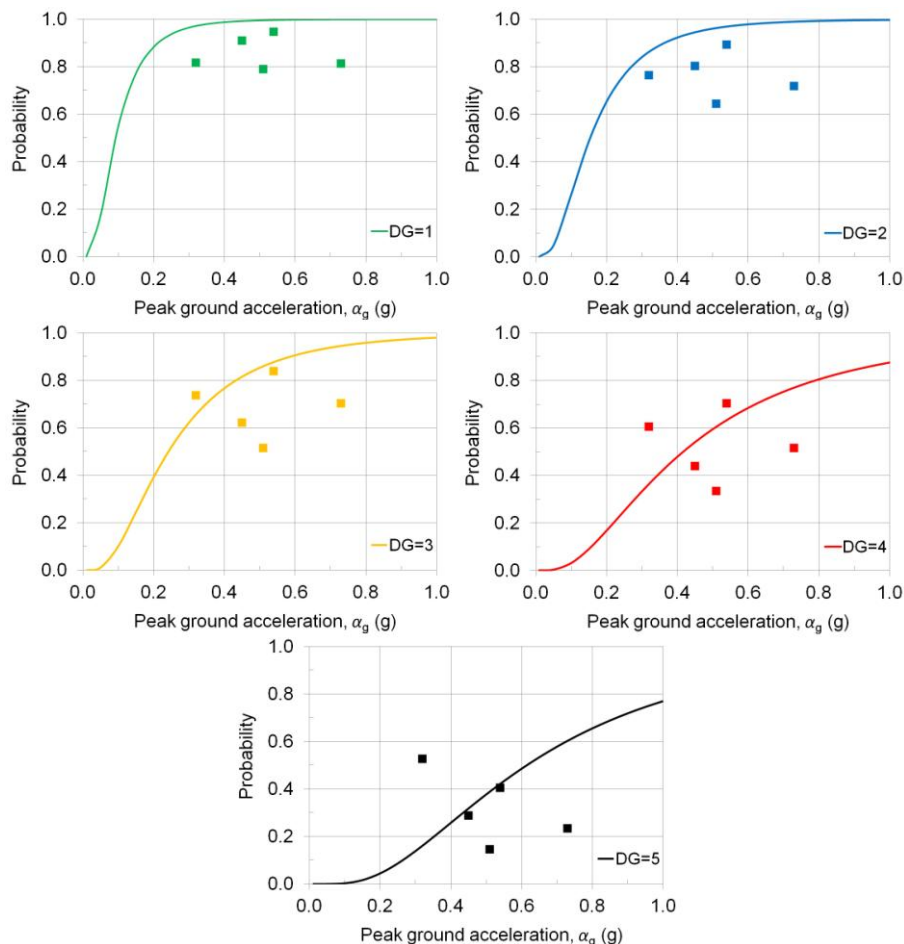


Fig. 14 Fragility curves of two-storey buildings with flexible floors and $h/l > 1$ compared to observed damage in the 1995 Aegion (GR) earthquake

majority of buildings in Aegion. The fragility curves were adjusted by multiplying the values of a_g calculated from Eq. (6) by 0.5, to reflect the spectral amplification calculated by Bouckovalas *et al.* (1999) for structures with fundamental period $T = 0.2$ sec. The numerical fragility curves are in fair agreement with the observed damage, particularly for the higher Damage Grades.

8.2 Comparison to existing fragility curves

Borzi *et al.* (2008) performed simplified pushover analyses assuming an equivalent single-degree-of-freedom system with elastic-perfectly plastic behaviour and a soft-storey mechanism, accounting for the variability of geometric and mechanical properties of buildings, to produce fragility curves for three damage states corresponding to "light damage" (no repair needed), "significant damage" (repair necessary but possibly not economically advantageous) and collapse.

In Fig. 15 the curves of Borzi *et al.* (2008) for two-storey buildings and only in-plane response and failure are compared to the ones from the present study for two-storey buildings with stiff

floors and the main component of the seismic action parallel to the interior walls (i.e. for $0.3E_x+E_y$), so as to minimise the effect of out-of-plane response. The two sets of curves are in fair agreement at the first Damage Grade (median PGA values 0.15g and 0.10g) but differ considerably at the two higher ones (median PGA of 0.23g and 0.44g for significant damage;

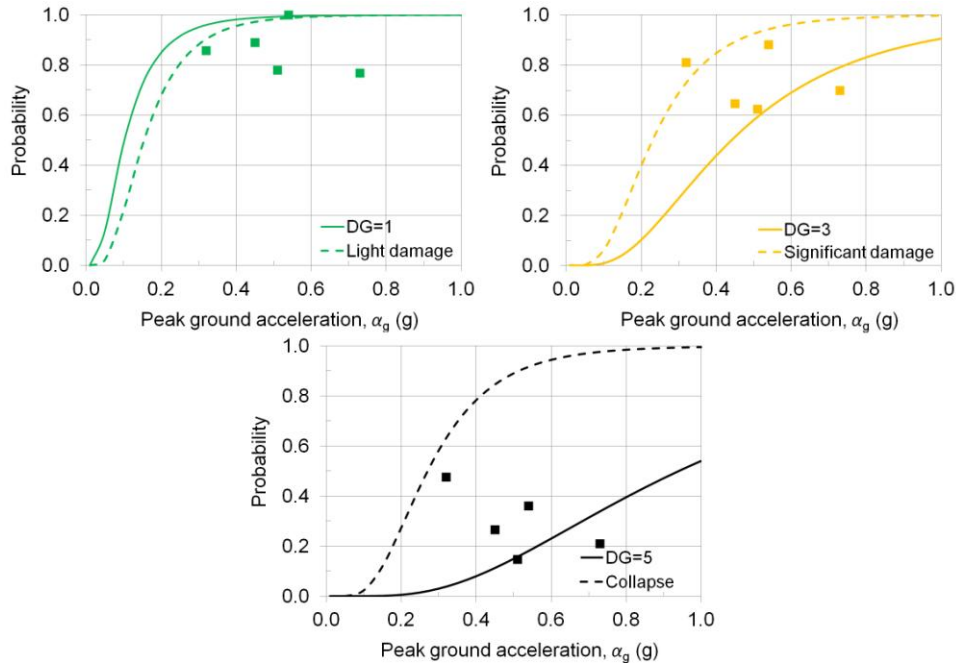


Fig. 15 Fragility curves of two-storey buildings with stiff floors, for the main seismic action component parallel to the interior walls, (continuous lines) compared to the fragility curves by Borzi *et al.* (2008) for two-storey buildings with high-quality masonry (dashed lines) and to the observed damage in the 1995 Aegion (GR) earthquake (squares)

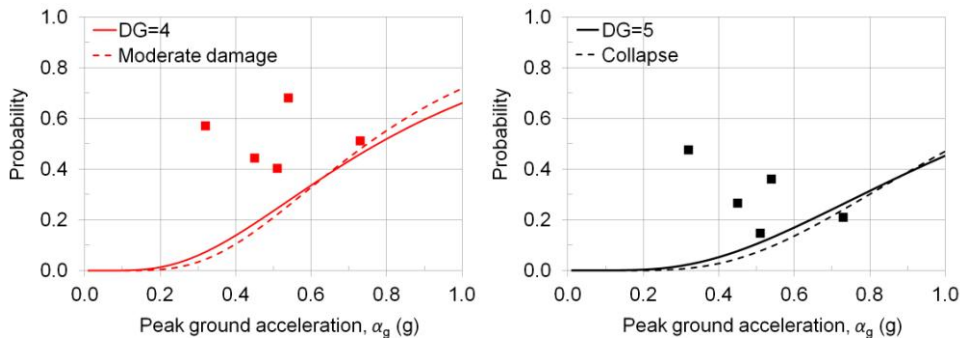


Fig. 16 Fragility curves of two-storey buildings with stiff floors for the main seismic action component parallel to the interior walls (continuous lines) compared to the fragility curves by Erberik (2008) for two-storey buildings with stiff floors and brick masonry (dashed lines) and to the observed damage in the 1995 Aegion (GR) earthquake (squares)

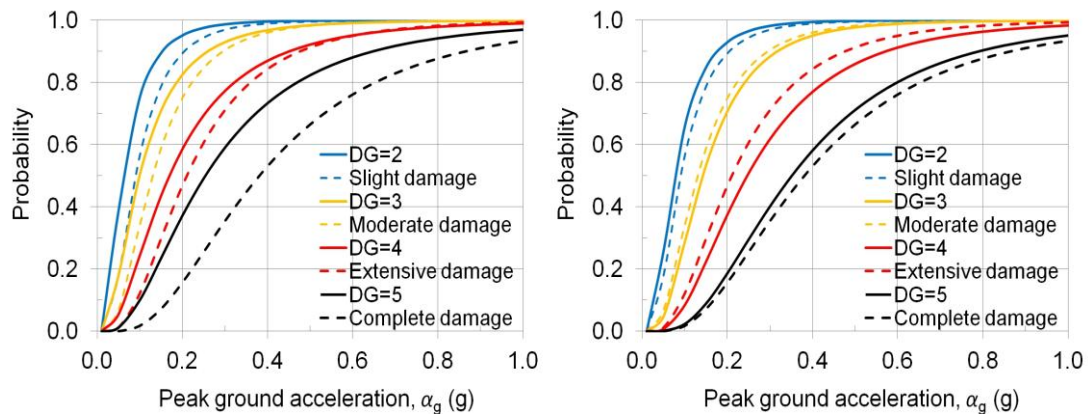


Fig. 17 Fragility curves of four-storey buildings with flexible floors (continuous lines) for combination of both seismic action components (left) or for the main component of the seismic action normal to the interior walls (right) compared to the HAZUS (FEMA 2010) fragility curves for mid-rise buildings without seismic design (dashed lines)

0.27g and 0.94g for collapse). The soft-storey mechanism with elastic perfectly-plastic behaviour in Borzi *et al.* (2008) results in significant increase of damage for small increase of PGA and consequently overestimates the building fragility. By contrast, the 3D FE analysis follows the gradual evolution of damage in the various parts of the building, as evidenced by the better agreement with the observed data, also depicted in Fig. 15.

The fragility curves in Erberik (2008) for two-storey Turkish masonry buildings with stiff floors are compared in Fig. 16 to the set of curves produced from the present study, correcting for the value $f_{wc} = 4$ MPa in Erberik (2008). The buildings were modelled in Erberik (2008) in 2D using wall panels and combined pushover analysis for the base shear capacity with time-history analysis to estimate the demand; fragility curves accounting for the variability in geometry, material strength and ground motion were produced for the limit states of moderate damage and collapse. The agreement of the curves from the two methodologies is satisfactory, also for other URM building classes not shown in Fig. 16 for brevity. The median values by Erberik (2008) are about the same as those calculated with the FE analysis for both Damage Grades. Witness in Fig. 16 how all fragility curves underestimate the observed damage, as they do not account for out-of-plane behaviour, whereas most buildings in Aegion had flexible floors and roofs.

Finally, the fragility curves for four-storey buildings with flexible floors are compared in Fig. 17 to the fragility curves of HAZUS (FEMA 2010) for mid-rise URM buildings not designed for earthquake resistance. HAZUS uses the capacity spectrum method to construct curves at four structural damage states: slight, moderate, extensive and complete. The agreement is good when the fragility curves are derived from FE analyses for both combinations of the seismic action components (Fig. 17 left). It further improves, mainly at the highest Damage Grade, when the fragility curves based on FE analyses for the main component of the seismic action parallel to the interior walls are examined (Fig. 17 right). The average difference of median values from the two methodologies reduces, from 27% in the first case, to 10% in the latter, consistent with a predominantly in-plane response of the HAZUS buildings.

9. Conclusions

Linear static FE analysis in 3D, with a nonlinear biaxial failure criterion for masonry, were performed to quantify and compare the seismic fragility of prototype stone masonry buildings, accounting for out-of-plane damage and failure modes, not captured by “equivalent” plane-frame models. As a matter of fact, such failure modes were found to markedly increase the vulnerability and reduce the relative influence of parameters such as the percentage of walls parallel to the seismic action, the pier aspect ratio, h/l , and the wall slenderness, h_{ef}/t_{ef} .

Fragility and damage curves were developed based on the results of over 1100 analyses, that cover the practical range of several geometric parameters, namely the number of storeys, percentage of side length in exterior walls taken up by openings, wall thickness, plan dimensions and number of interior walls, type of floor, pier height-to-length ratio and the direction of the seismic action. The Intensity Measure used to describe the seismic fragility is the effective spectral acceleration (convertible to PGA, if a dependence of the force-reduction- or behaviour-factor, q , on Damage Grade is assumed), divided by the masonry compressive strength. The fragility curves agree well with the damage statistics from the 1995 Aegion (GR) earthquake. Moreover, they are in good agreement with fragility curves in the literature developed with other modelling and analysis methods, but do better by accounting for the marked out-of-plane response of buildings with flexible floors, ignored in most past fragility studies.

The reduction of the vulnerability of buildings with stiff floors and roof and of lower-rise buildings was quantified. Similarly for the increase in vulnerability due to higher wall slenderness and pier aspect ratio, mainly for stiff floors. The amount by which a higher percentage of load-bearing walls is beneficial for seismic fragility was also estimated. Although these effects were qualitatively known or expected, they have been quantified here in generic terms, over a range of parameters that covers almost all practical cases.

Acknowledgements

The research leading to these results received funding from the European Community's 7th Framework Programme (FP7/2007-2013) under grant agreement n° 244061 (SYNER-G).

References

- Borzi, B., Crowley, H. and Pinho, R. (2008), “Simplified pushover-based earthquake loss assessment (SP-BELA) method for masonry buildings”, *Int. J. Archit. Herit.*, **2**(4), 353-376.
- Bothara, J.K., Dhakal, R.P. and Mander, J.B. (2010), “Seismic performance of an unreinforced masonry building: An experimental investigation”, *Earthq. Eng. Struct. Dyn.*, **39**(1), 45-68.
- Bouckovalas, G.D., Gazetas, G. and Papadimitriou, A.G. (1999), “Geotechnical aspects of the 1995 Aegion (Greece) earthquake”, *Proceedings of the 2nd International Conference on Earthquake Geotechnical Engineering*, Lisbon, Portugal, June.
- Cattari, S., Curti, E., Giovinazzi, S., Lagomarsino, S., Parodi, S. and Penna, A. (2004), “Un modello meccanico per l'analisi di vulnerabilità del costruito in muratura a scala urbana”. *XI Congresso Nazionale “L'ingegneria Sismica in Italia”*, Genoa, Italy, January.
- CEN (2004), *EN 1998-1 Eurocode 8: Design of structures for earthquake resistance - Part 1: General rules, seismic actions and rules for buildings*, Brussels.

- CEN (2005), *EN 1996-1-1 Eurocode 6: Design of masonry structures - Part 1-1: General rules for reinforced and unreinforced masonry structures*, Brussels.
- Colombi, M., Borzi, B., Crowley, H., Onida, M., Meroni, F. and Pinho, R. (2008), "Deriving vulnerability curves using Italian earthquake damage data", *Bull. Earthq. Eng.*, **6**(3), 485-504.
- D'Ayala, D., Spence, R., Oliveira, C. and Pomonis, A. (1997), "Earthquake loss estimation for Europe's historic town centres", *Earthq. Spectra*, **13**(4), 773-793.
- Doherty, K.T., Griffith, M.C., Lam, N. and Wilson, J. (2002), "Displacement-based seismic analysis for out-of-plane bending of unreinforced masonry wall", *Earthq. Eng. Struct. Dyn.*, **31**(4), 833-850.
- Erberik, M.A. (2008), "Generation of fragility curves for Turkish masonry buildings considering in-plane failure modes", *Earthq. Eng. Struct. Dyn.*, **37**(3), 387-405.
- FEMA (2010), *Hazus MH MR5 technical manual*, Federal Emergency Management Agency, Washington, USA.
- Frankie, T.M., Gencturk, B. and Elnashai, A.S. (2013), "Simulation-based fragility relationships for unreinforced masonry buildings", *ASCE J. Struct. Eng.*, **139**(3), 400-410.
- Griffith, M.C., Magenes, G., Melis, G. and Picchi, L. (2003) "Evaluation of out-of-plane stability of unreinforced masonry walls subjected to seismic excitation", *J. Earthq. Eng.*, **7**(SP1), 141-169.
- Grünthal, G. (1998), *European Macroseismic Scale 1998 (EMS-98)*, Centre Européen de Géodynamique et de Séismologie, Luxembourg, Luxembourg.
- Kappos, A.J., Panagopoulos, G., Panagiotopoulos, C. and Penelis, G. (2006), "A hybrid method for the vulnerability assessment of R/C and URM buildings", *Bull. Earthq. Eng.*, **4**(4), 391-413.
- Karababa, F.S. and Pomonis, A. (2011), "Damage data analysis and vulnerability estimation following the August 14, 2003 Lefkada Island, Greece, Earthquake", *Bull. Earthq. Eng.*, **9**(4), 1015-1046.
- Karantoni, F.V. and Fardis, M.N. (1992), "Computed versus observed seismic response and damage of masonry buildings", *ASCE J. Struct. Eng.*, **118**(7), 1804-1821.
- Karantoni, F.V., Fardis, M.N., Vintzeleou, E. and Harisis, A. (1993), "Effectiveness of seismic strengthening interventions", *Proceedings of the IABSE Symposium on Structural Preservation of the Architectural Heritage*, Rome, Italy, September.
- Karantoni, F.V. and Fardis, M.N. (2005), "Damage to masonry buildings due to the Aegion, (Gr) 1995 Earthquake", *Proceedings of the 9th International Conference on Structural Studies, Repairs and Maintenance of Heritage Architecture*, Malta, June.
- Lagomarsino, S. and Giovinazzi, S. (2006), "Macroseismic and mechanical models for the vulnerability and damage assessment of current buildings", *Bull. Earthq. Eng.*, **4**(4), 415-443.
- Lang, K. and Bachmann, H. (2004), "On the seismic vulnerability of existing buildings: a case study of the city of Basel", *Earthq. Spectra*, **20**(1), 43-66.
- Magenes, G. (2010), "Earthquake resistant design of masonry structures: rules, backgrounds, latest findings", *Proceedings of the 8th International Masonry Conference*, Dresden, Germany, July.
- Magenes, G. and Calvi, G.M. (1997), "In-plane seismic response of brick masonry walls", *Earthq. Eng. Struct. Dyn.*, **26**(11), 1091-1112.
- Ottosen, N. (1977), "A failure criterion for concrete", *ASCE J. Eng. Mech.*, **103**(4), 527-535.
- Page, A.W. (1983), "The strength of brick masonry under biaxial tension-compression", *Int. J. Mason. Constr.*, **3**(1), 26-31.
- Pagnini, L.C., Vicente, R., Lagomarsino, S. and Varum, H. (2011), "A mechanical model for the seismic vulnerability assessment of old masonry buildings", *Earthq. Struct.*, **2**(1), 25-42.
- Park, J., Towashiraporn, P., Craig, J.I. and Goodno B.J. (2009) "Seismic fragility analysis of low-rise unreinforced masonry structures", *Eng. Struct.*, **31**(1), 125-137.
- Pasticier, L., Amadio, C. and Fragiaco, M. (2008), "Non-linear seismic analysis and vulnerability evaluation of a masonry building by means of the SAP2000 V.10 code", *Earthq. Eng. & Struct. Dyn.*, **37**(3), 467-485.
- Penelis, G.G., Kappos, A.J. and Stylianidis, K.C. (2002), *Unreinforced masonry buildings – 1st level analysis*, RISK-UE report, University of Thessaloniki, Thessaloniki, Greece.

- Rota, M., Penna, A. and Strobbia, C.L. (2008), "Processing Italian damage data to derive typological fragility curves", *Soil Dyn. Earthq. Eng.*, **28**(10-11), 933-947.
- Rota, M., Penna, A. and Magenes, G. (2010), "A methodology for deriving analytical fragility curves for masonry buildings based on stochastic nonlinear analyses", *Eng. Struct.*, **32**(5), 1312-1323.
- Yi, T., Moon, F., Leon, R.T. and Kahn, L.F. (2006), "Lateral load tests on a two-story unreinforced masonry building", *ASCE J. Struct. Eng.*, **132**(5), 643-652.

SA